Superposed epoch analysis of the ionospheric convection evolution during substorms: IMF B_Y dependence

A. Grocott,[1] S. E. Milan,[1] T. K. Yeoman,[1] N. Sato,[2] A. S. Yukimatu,[2] and J. A. Wild[3]

Received 28 May 2010; revised 9 July 2010; accepted 26 July 2010; published 26 October 2010.

[1] We present superposed epoch analyses of the average ionospheric convection response in the northern and southern hemispheres to magnetospheric substorms occurring under different orientations of the interplanetary magnetic field (IMF). Observations of the ionospheric convection were provided by the Super Dual Auroral Radar Network (SuperDARN) and substorms were identified using the Far Ultraviolet (FUV) instrument on board the Imager for Magnetopause-to-Aurora Global Exploration (IMAGE) spacecraft. We find that during the substorm growth phase the expected IMF B_Y-dependent dawn-dusk asymmetry is observed over the entire convection pattern, but that during the expansion phase this asymmetry is retained only in the polar cap and dayside auroral zone. In the nightside auroral zone the convection is reordered according to the local substorm electrodynamics with any remaining dusk-dawn asymmetry being more closely related to the magnetic local time of substorm onset, itself only weakly governed by IMF B_Y. Owing to the preponderance of substorms occurring just prior to magnetic midnight, the substorm-asymmetry tends to be an azimuthal extension of the dusk convection cell across the midnight sector, a manifestation of the so-called "Harang discontinuity." This results in the northern (southern) hemisphere nightside auroral convection during substorms generally resembling the expected pattern for negative (positive) IMF B_Y. When the preexisting convection pattern in the northern (southern) hemisphere is driven by positive (negative) IMF B_Y, the nightside auroral convection changes markedly over the course of the substorm to establish this same "Harang" configuration.

Citation: Grocott, A., S. E. Milan, T. K. Yeoman, N. Sato, A. S. Yukimatu, and J. A. Wild (2010), Superposed epoch analysis of the ionospheric convection evolution during substorms: IMF B_Y dependence, *J. Geophys. Res.*, *115*, A00I06, doi:10.1029/2010JA015728.

1. Introduction

[2] Solar wind-magnetosphere coupling is the dominant process driving high-latitude ionospheric convection. As a result, global observations of the large-scale ionospheric convection pattern, such as those afforded to us by the Super Dual Auroral Radar Network (SuperDARN) [*Greenwald et al.*, 1995; *Chisham et al.*, 2007], are often used to investigate the nature of this interaction [e.g., *Ruohoniemi and Greenwald*, 1996; *Ruohoniemi and Baker*, 1998; *Ruohoniemi and Greenwald*, 2005]. When reconnection occurs between the interplanetary and terrestrial magnetic fields convection is excited in the dayside ionosphere [e.g., *Etemadi et al.*, 1988; *Todd et al.*, 1988; *Ruohoniemi et al.*, 1993; *Provan et al.*, 2005]. During intervals of southward IMF, when closed terrestrial field lines reconnect, open flux is created and antisunward convection is driven across the polar cap [e.g., *Siscoe and Huang*, 1985; *Freeman and Southwood*, 1988; *Cowley and Lockwood*, 1992; *Milan et al.*, 2003]. When the IMF also has a dusk-dawn (B_Y) component this gets imparted to the antisunward flow of open flux via the Svalgaard-Mansurov effect [*Jørgensen et al.*, 1972; *Svalgaard*, 1973; *Cowley*, 1981]. The average nature of the ionospheric flow patterns associated with southward IMF ($B_Z < 0$) for various orientationsof B_Y, as determined from SuperDARN observations by *Ruohoniemi and Greenwald* [2005], are illustrated in Figure 1.

[3] The instantaneous nature of the ionospheric convection patterns differs from these statistical averages owing to the time-dependent nature of the system. This time-dependency was discussed in terms of the large-scale dynamics by *Cowley and Lockwood* [1992] and subsequently extended to include finer substructures related to, for example, IMF B_Y-related Birkeland currents and ionospheric conductivity gradients [*Sandholt and Farrugia*, 2007, 2009; *Wang et al.*, 2010; *Sandholt et al.*, 2010]. Whereas open flux creation and the

[1]Department of Physics and Astronomy, University of Leicester, Leicester, UK.
[2]Space and Upper Atmospheric Sciences Research Group, National Institute of Polar Research, Research Organization of Information and Systems, Tachikawa, Japan.
[3]Department of Physics, Lancaster University, Lancaster, UK.

0148-0227/10/2010JA015728

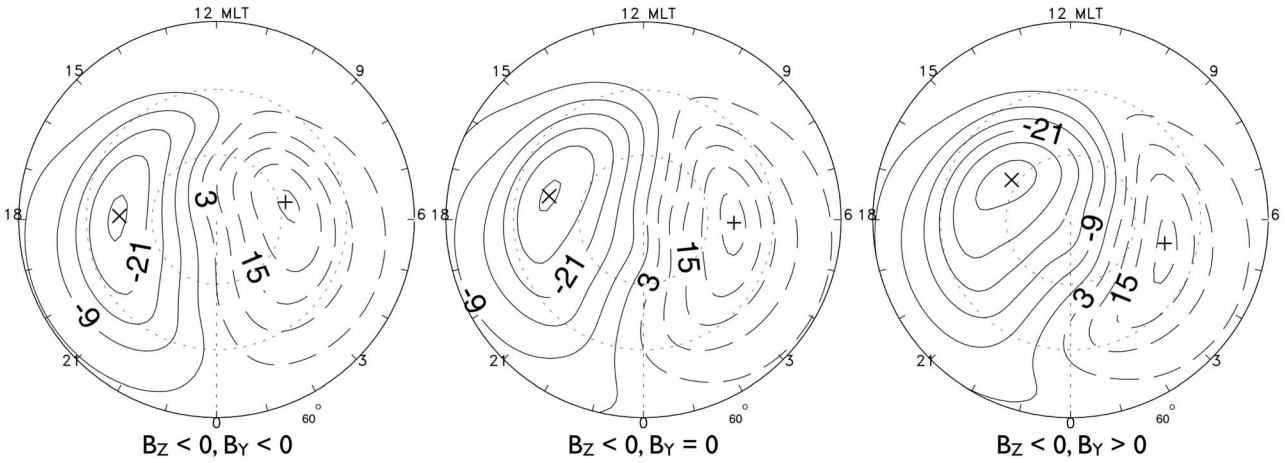

Figure 1. The statistical convection patterns from *Ruohoniemi and Greenwald* [2005] for southward IMF ($B_Z < 0$), for various orientations of B_Y for the 5–10 nT interval of IMF magnitude.

subsequent expansion of the polar cap is largely governed by the interaction with the IMF, it is processes internal to the magnetosphere that are ultimately responsible for the closure of this accumulated open flux and its return to the dayside [e.g., *Dungey*, 1961; *Baker et al.*, 1996]. Theoretical considerations imply that nightside reconnection should drive coupled ionospheric-magnetospheric convection in much the same way as dayside reconnection, given that a change in open flux topology occurs in both cases and will thus excite convection to redistribute flux about the polar cap [*Cowley and Lockwood*, 1992, 1996]. Recent studies using SuperDARN have revealed that convection is indeed driven in the nightside ionosphere during intervals of magnetotail activity both during substorm times [e.g., *Grocott et al.*, 2002; *Provan et al.*, 2004; *Grocott et al.*, 2006] and nonsubstorm times [e.g., *Grocott et al.*, 2003, 2007]. However, the nature of this convection is somewhat variable and not always related to the instantaneous upstream interplanetary conditions that so strongly govern the dayside phenomenology.

[4] When the IMF is directed northward, but with a significant B_Y component, low-latitude dayside reconnection is maintained at a rate which is sufficient to gradually inflate the tail, but insufficient to drive the substorm cycle [e.g., *Sandholt et al.*, 1998a, 1998b; *Grocott et al.*, 2003]. During extended intervals of such IMF orientations bursts of fast azimuthal flow have been observed in the nightside ionosphere in association with modest contractions of the polar cap. *Milan et al.* [2005] coined the term "Tail Reconnection during IMF-Northward, Non-substorm Intervals" (TRINNIs) to describe this phenomenon, which recurs on timescales of tens of minutes, and acts to balance the low-level open flux creation at the dayside. The lack of associated substorm signatures such as geosynchronous particle injections and global auroral expansions implies that this reconnection is occurring at a more distant neutral line, rather than the near-Earth neutral line which is activated at substorm onset. The dependence of the orientation of TRINNI flows on IMF B_Y, as well as the interhemispheric asymmetry which they display, has led several authors including *Nishida et al.* [1995, 1998] and *Grocott et al.* [2005, 2007] to suggest a mechanism for their generation based on the idea of magnetic field reconfiguration following reconnection in a twisted tail. The strong IMF B_Y control of these nightside flows is illustrated in Figure 2 which shows the average nature of TRINNI flows derived from a statistical investigation by *Grocott et al.* [2008]. These results clearly illustrate that under certain circumstances the influence of IMF B_Y can dominate the tail dynamics and corresponding nightside ionosphere to a similar extent to that seen on the dayside.

[5] When the IMF is directed southward, as is the case for the average patterns shown in Figure 1, the coupled ionosphere-magnetosphere dynamics are dominated by the substorm cycle. However, in the studies of *Ruohoniemi and Greenwald* [1996, 2005] no account was taken of substorm phase such that the average patterns presented will contain a mixture of substorm and nonsubstorm behavior, which limits our understanding of the system. There have been mixed reports regarding the nature of the ionospheric convection that accompanies substorms, with studies using SuperDARN having provided evidence for both the excitation [e.g., *Grocott et al.*, 2002, 2006; *Provan et al.*, 2004] and reduction [e.g., *Yeoman et al.*, 2000a; *Lyons et al.*, 2001; *Bristow and Jensen*, 2007] of the flows following substorm onset. In a recent study *Grocott et al.* [2009] shed some light on this apparent inconsistency by conducting a superposed epoch analysis of the ionospheric convection evolution during substorms grouped by their onset latitude. They found that ionospheric convection is indeed enhanced following substorm onset, but that the electrodynamics are strongly modified by the ionospheric conductivity within the auroral bulge, which is itself dependent on onset latitude [*Milan et al.*, 2009].

[6] If it is true, therefore, that the substorm process strongly controls the nature of the nightside ionospheric convection then it remains to be determined whether this influence, or that of the prevailing IMF conditions, is the dominant influence, or, what is the effect of the superposition of both. *Yeoman et al.* [2000b], for example, presented interhemispheric observations of the nightside electric field response to changes in the IMF around the time of a substorm pseudobreakup. They found that although the convection exhibited the expected IMF B_Y interhemispheric asymmetries outside of the pseudobreakup interval, the electrodynamics associated with the pseudobreakup itself

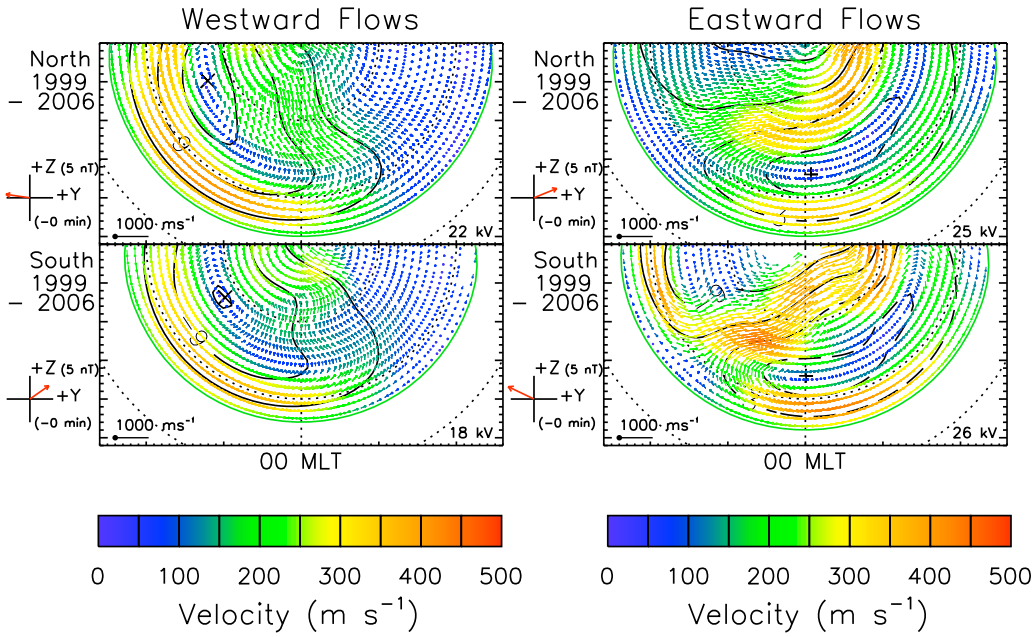

Figure 2. Streamlines and flow vectors of ionospheric convection derived from SuperDARN velocity measurements shown on geomagnetic latitude-MLT grids, with midnight at the bottom and dusk to the left. The four plots show average nightside ionospheric convection patterns in the northern and southern hemispheres for 'TRINNI' intervals as described by *Grocott et al.* [2008]. The arrow in the bottom left indicates the average magnitude and orientation of the interplanetary magnetic field in the Y-Z plane.

appeared to be reasonably conjugate in both hemispheres. This suggests that substorm-like activity will, to some extent, inhibit the asymmetries typically associated with IMF B_Y. *Liou and Ruohoniemi* [2006a, 2006b], on the other hand, found that the preexisting solar wind-driven convection resulting from, in particular, the IMF B_Y influence in fact controls the substorm onset and the evolution of the auroral bulge. In the present study we therefore investigate the effect of substorm activity on the nature of the nightside ionospheric convection for different orientations of IMF B_Y, by performing a similar superposed epoch analysis as in the work of *Grocott et al.* [2009]. We find that although the magnetic local time of substorm onset is weakly dependent on IMF B_Y, the substorm electrodynamics impose a dusk-dawn asymmetry that is largely independent of IMF B_Y and which modifies the preexisting IMF B_Y-dominated convection pattern in the auroral zone.

2. Data Analysis

[7] In common with the study of *Grocott et al.* [2009] we have used data from the *Frey et al.* [2004] list of substorms, derived from auroral data from the IMAGE FUV instrument [*Mende et al.*, 2000b, 2000a], to produce a set of 1979 northern hemisphere isolated onsets [*Wild and Grocott*, 2008]. Onset time is defined as the time of the FUV image in which a clear local brightening of the aurora occurred, an onset only being included if that brightening then proceeded to expand to the poleward boundary of the auroral oval and spread azimuthally in local time for at least 20 min [*Frey et al.*, 2004]. For the purposes of our study, a substorm onset was only accepted as an isolated event if at least 2 h had passed since the previous onset. The distribution of onset locations in magnetic latitude-magnetic local time for these events is reproduced from *Grocott et al.* [2009] in Figure 3a. Figure 3b presents the IMF clock angle distribution, determined using observations from the Advanced Composition Explorer (ACE) spacecraft [*Stone et al.*, 1998; *Smith et al.*, 1998], versus onset-MLT. Here, the IMF clock angle, θ, is defined as the angle between the Geocentric Solar Magnetic (GSM) z-direction (northward) and the projection of the IMF vector onto the y–z plane. Owing to the ongoing uncertainty surrounding the time taken for changes in IMF orientation to be observed in the nightside ionosphere [e.g., *Ruohoniemi and Greenwald*, 1998; *Watanabe et al.*, 2000; *Yeoman et al.*, 2000b; *Yu and Ridley*, 2009; *Milan et al.*, 2010] we decided it was not sufficient to simply use the IMF orientation at the time of substorm onset to determine θ. Instead, we used 2 h running mean filtered IMF vectors to remove rapid fluctuations in the data, to account for the uncertainty in propagating the ACE observations to the ionosphere and to allow for some propagation delay through the magnetosphere to the nightside ionosphere. We then took the mean value of these filtered IMF vectors for the 2 h interval centered on the time of substorm onset. Figure 3b thus shows that the peak in substorm occurrence corresponds to $\theta \approx \pm 100°$. In other words, most substorms occur when there is a dominant IMF B_Y-component which is consistent with the average orientation of the Parker spiral field [*Parker*, 1963].

[8] Any relationship between θ and onset MLT is, however, marginal at best. There is some evidence of a small (~1–2 h) offset between the grouping of high occurrence for the positive clock angle regime and that for the negative

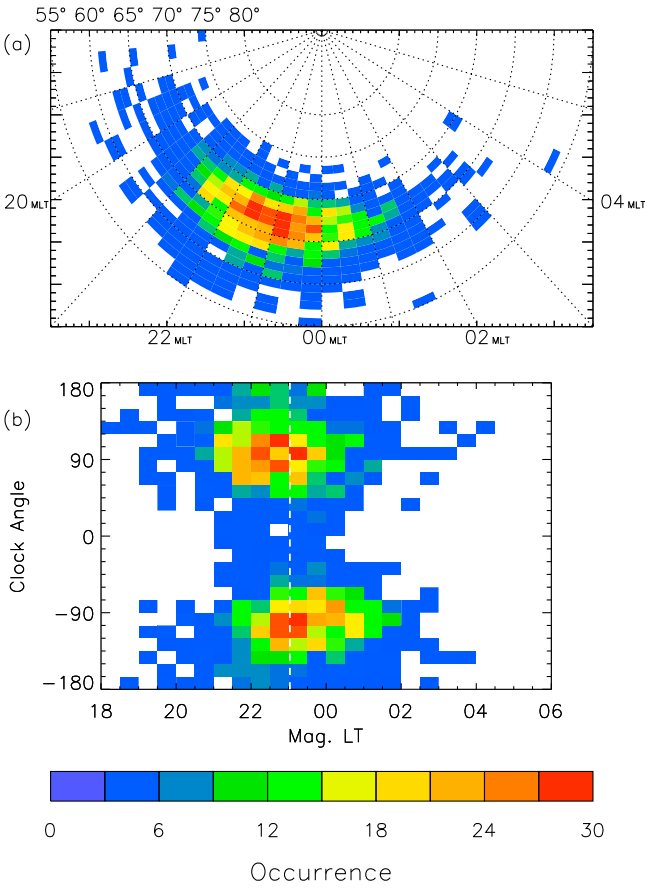

Figure 3. (a) The locations of northern hemisphere isolated substorm onsets, observed by the FUV instrument on-board the IMAGE satellite, presented in magnetic latitude–magnetic local time coordinates and (b) magnetic local times versus IMF clock angle for the substorm onsets shown in Figure 3a. The occurrence of substorms within each bin is color coded according to the scale at the bottom.

clock angle regime, but nothing comparable to the clock angle related dusk-dawn asymmetry evident in, for example, the TRINNI flows shown in Figure 2. This small clock angle dependence of substorm onset location is consistent with the study of *Yeoman et al.* [2000b] discussed above, and also with previous conjugate interhemispheric auroral observations of substorms [e.g., *Østgaard et al.*, 2004, 2007]. These latter studies revealed that the most significant IMF B_Y-control of substorm onset location is the introduction of a small offset in MLT between the northern and southern auroral onsets. This offset is given by $\Delta\text{MLT} = -0.017\theta + 3.44$ [*Østgaard et al.*, 2004], where ΔMLT is positive for a southern onset location dawnward of the northern location, and was defined for the IMF clock angle range $90° < \theta < 300°$. The ΔMLTs for the substorms used in the present study have been calculated and are discussed in section 3.

[9] In order to investigate more generally how the convection responds to substorms in the presence of different preexisting IMF orientations we have therefore performed a superposed epoch analysis of ionospheric convection data from SuperDARN via a similar method as *Grocott et al.* [2009]. For the purposes of this study, however, we have taken a single onset latitude bin of 65°–67°. This is wider than the 1° bins used in the *Grocott et al.* [2009] study, but necessary to maintain a representative number of events in subsequent bin divisions. We have chosen substorms with onsets in this latitude range for a combination of reasons: (1) they need to be of sufficiently high latitude to be well observed by the latitudinally restricted fields-of-view of the SuperDARN radars and (2) they should be at the lowest latitude end of the range satisfying (1) such that they are of the highest intensity possible [*Milan et al.*, 2009] and therefore likely to produce the strongest observable effect in the ionosphere. We then further subdivided this set of events based on our 2 h IMF B_Y mean values and selected substorms where this was either less than −2 nT or greater than +2 nT. Four sets of superposed epoch average convection patterns were then derived from 1 h prior, to 1.5 h after substorm onset, for each of the two IMF B_Y bins in the northern and southern hemispheres. These patterns were derived by median filtering the local velocity measurements in each 2 min interval, for all events in a bin, and then applying the global Map Potential fitting algorithm [*Ruohoniemi and Baker*, 1998; *Shepherd and Ruohoniemi*, 2000]. The number of median filtered vectors, N, used in the fit for each 2 min interval varied between 1320 and 2013. Typically ~150–200 vectors are present in an individual 2 min SuperDARN convection map meaning that the superposed epoch analysis affords us an order of magnitude improvement over an individual event in the number of measurements that are used to constrain the fit.

3. Observations

[10] Selected sets of average ionospheric convection patterns from key times during the substorm cycle, derived from the superposed epoch analysis of SuperDARN observations discussed in section 2, are shown in Figure 4. Five sets of convection patterns are shown, from 48 mins (Figure 4a), 14 mins (Figure 4b) and 2 mins (Figure 4c) prior to substorm onset, and 30 mins (Figure 4d) and 66 mins (Figure 4e) after substorm onset. Four patterns are shown in each case: two from each of the northern (Figures 4a–4e, top) and southern (Figures 4a–4e, bottom) hemispheres, for each of the two cases of IMF B_Y (negative in Figures 4a (left), 4b (left), 4c (left), 4d (left), and 4e (left) and positive in Figures 4a (right), 4b (right), 4c (right), 4d (right), and 4e (right)). For convenience, these four patterns will henceforth be referred to as N−, N+, S− and S+, in reference to the hemisphere and sign of IMF B_Y. The data are shown on a magnetic latitude-magnetic local time grid with noon to the top and dusk to the left. The concentric dotted circles represent lines of constant magnetic latitude in 10° increments from 60° to the pole. Southern hemisphere data are shown plotted on the same northern hemisphere grid, mapped according to the Altitude Adjusted Corrected GeoMagnetic (AACGM) coordinate system [*Baker and Wing*, 1989] as is conventional for presenting SuperDARN data. The velocity vectors are shown with a dot at the origin and are color coded according to the color bar on the right. The number of vectors, N, is displayed at the top of each plot. The black + near midnight indicates the average northern hemisphere position of substorm onset

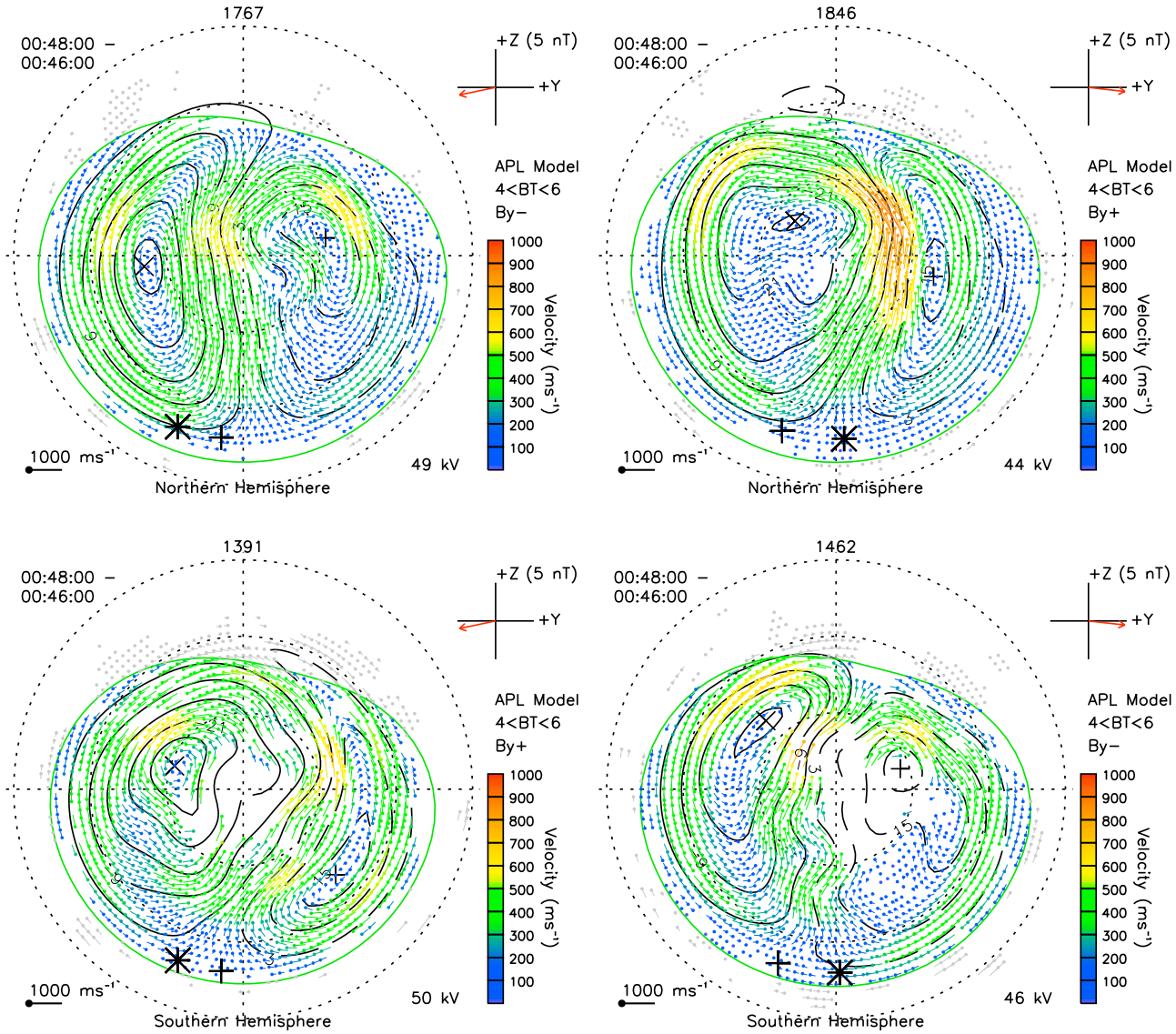

Figure 4a. Average ionospheric convection patterns from 48 mins prior to substorm onset from the (top) northern and (bottom) southern hemisphere for the case of (left) negative and (right) positive IMF B_Y. The data are shown on a magnetic latitude-magnetic local time grid with noon to the top and dusk to the left. The concentric dotted circles represent lines of constant magnetic latitude from 60° to the pole. The black + near midnight indicates the average northern hemisphere position of substorm onset (from the substorm database used in this study) and the black * the corresponding *Østgaard et al.* [2004] predicted southern hemisphere location.

(from the substorm database used in this study). The black * represents the corresponding [*Østgaard et al.*, 2004] predicted Southern Hemisphere location as discussed in section 2.

[11] In Figure 4a, during the early growth phase, the expected asymmetry due to dayside reconnection with a B_Y-dominated IMF is evident in the convection patterns, i.e., the eastward sense of the polar cap flow for the N− and S+ patterns and the westward sense for the N+ and S− patterns. A modest (~1 h) difference in MLT between the average northern hemisphere onset location is evident between the $B_Y < -2$ nT and $B_Y > 2$ nT cases, as expected, with a similar, if slightly larger difference between the predicted southern hemisphere onset MLTs. As the growth phase progresses (Figure 4b) the flows intensify significantly and the asymmetry between the dusk and dawn convection cells increases.

[12] By about the time of substorm onset (Figure 4c) the nature of the nightside portions of the convection patterns has begun to change. Firstly, in all four cases, a low flow region (dark blue vectors) has developed at ~70° in the flow reversal region stretching from approximately midnight into the dusk cell. In the northern hemisphere the widest (in latitude) portion of this region is colocated with the average onset location (+) and in the southern hemisphere it is colocated with the predicted average southern hemisphere onset location (*). This is consistent with previous observa-

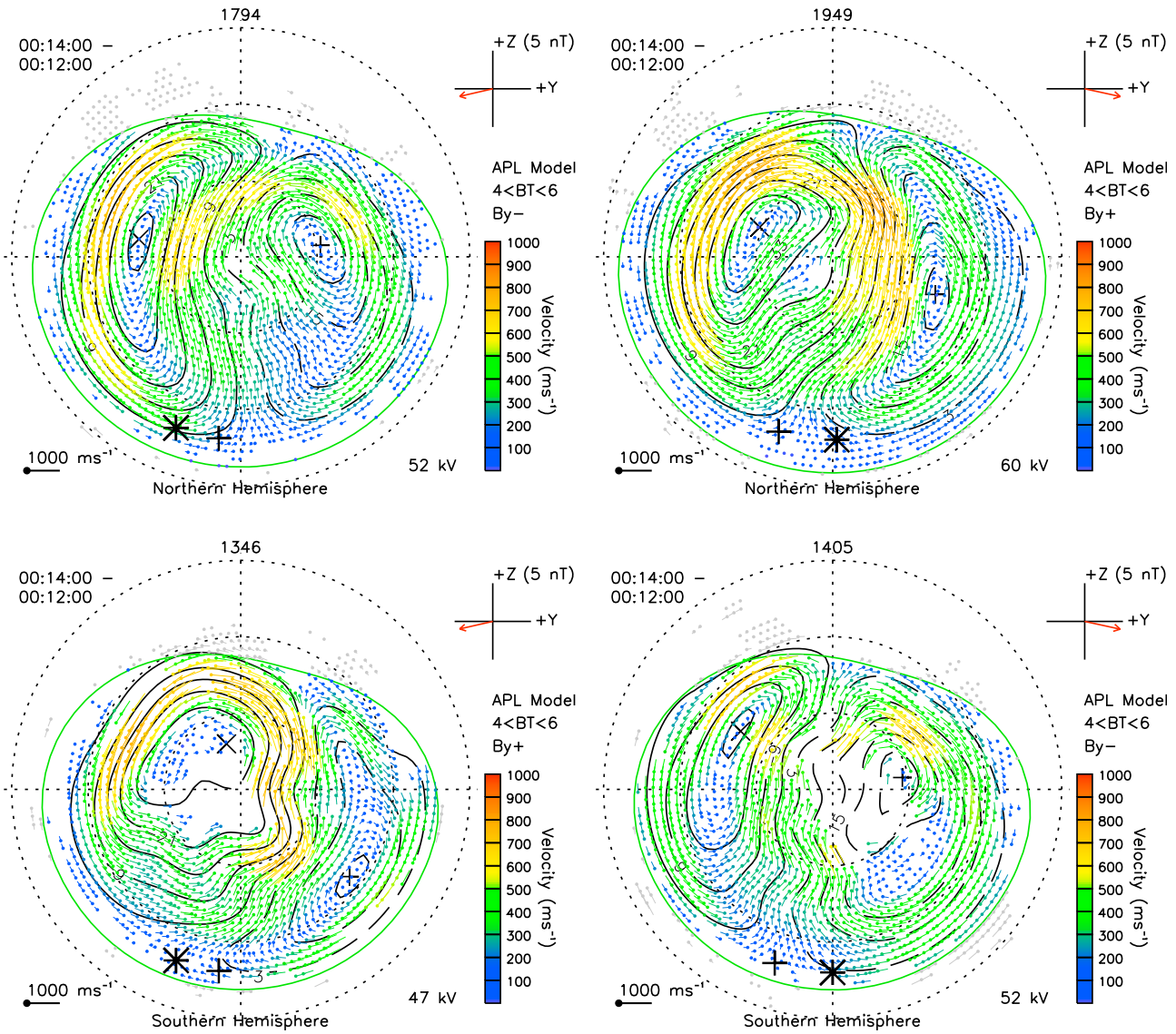

Figure 4b. Average ionospheric convection patterns from 14 mins prior to substorm onset.

tions of electric field suppression in the auroral bulge [*Morelli et al.*, 1995; *Yeoman et al.*, 2000a; *Grocott et al.*, 2006; *Milan et al.*, 2009]. Looking, in particular, at the N+ and S− patterns, it appears that the development of this low flow region occurs in concert with a bifurcation of the dusk return flows. One channel of return flow exists poleward of ~70°, associated with a westward flow reversal. Equatorward of this an eastward convection reversal occurs in the low flow region (most notably evident in the N+ pattern but subtly evident in the S− pattern also), and then further equatorward a second channel of return flow is associated with a lower-latitude westward flow reversal at ~65°.

[13] Figure 4d shows the situation 30 mins into the expansion phase. By this time the "double reversal" in the auroral zone convection is now more clearly evident in the S− pattern, whilst remaining apparent in the N+ pattern. The N− pattern also appears to exhibit this double reversal and whilst it is not so clear for S+, this pattern has nevertheless developed a more pronounced east-west reversal just premidnight. This evolution of the nightside convection in all cases has resulted in patterns which, although exhibiting the expected IMF B_Y-asymmetries in the polar cap, now appear to have almost identical forms in the nightside auroral zone, irrespective of the preexisting influence of B_Y.

[14] Lastly, Figure 4e serves to illustrate the longevity of these features in the convection; more than 1 h after substorm onset the basic nature of the convection patterns is the same. There have also been some additional interhemispheric asymmetries introduced which do not appear to be directly related to IMF B_Y. For example, the low-flow region in the dusk flow reversal zone is much wider in the southern hemisphere, where the flows are also generally of lower magnitude. These differences may be significant to

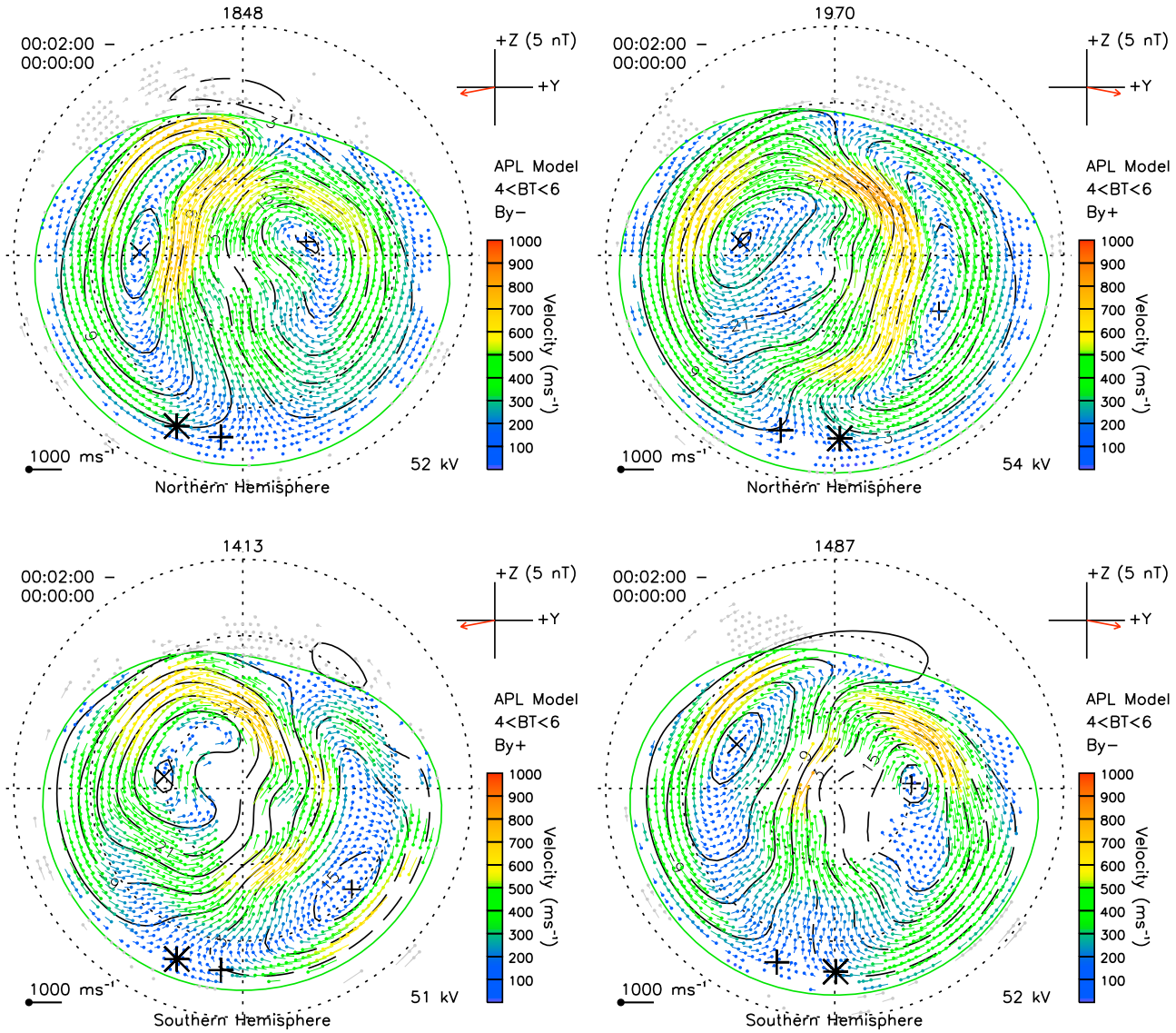

Figure 4c. Average ionospheric convection patterns from 2 mins prior to substorm onset.

our understanding of the smaller-scale physics of the magnetosphere-ionosphere coupling but discussion of these is beyond the scope of the present paper.

4. Discussion

[15] We have presented superposed epoch analyses of the average ionospheric convection response to magnetospheric substorms occurring under different orientations of IMF B_Y. The clear evidence for an IMF B_Y related dusk-dawn asymmetry in the convection during the growth phase suggests that the IMF orientation is governing the nature of the convection pattern during this time. This is consistent with what we understand about the solar wind-magnetosphere interaction and the excitation of twin-vortex convection by low-latitude reconnection during intervals of southward, but B_Y-dominated IMF [e.g., *Dungey*, 1961; *Jørgensen et al.*, 1972; *Fairfield*, 1977]. In the traditional picture, discussed by *Lockwood* [1991], this B_Y-asymmetry is evident over the entire convection pattern, both in the polar cap and in the auroral zones. The existence of this dusk-dawn asymmetry in the nightside auroral zone in particular is related to magnetosphere-ionosphere coupling, and the fact that the IMF penetrates into the geomagnetic tail, such that its sense is retained on closed flux tubes within the plasma sheet [e.g., *Cowley*, 1981]. The case studies of *Liou and Ruohoniemi* [2006a, 2006b] appear to support the idea that this concept holds true for substorms and that, in fact, the pre-existing IMF-controlled convection actually governs the auroral evolution of the substorm. Our results, on the other hand, suggest that during the substorm process the effects of IMF B_Y are inhibited to a large extent, consistent with the findings of *Yeoman et al.* [2000b] discussed in section 1. We discuss this apparent contradiction and suggest a mechanism to explain our observations below.

[16] First it is worth discussing these results in relation to previous observations of substorm electrodynamics. A common feature often observed during substorms is the

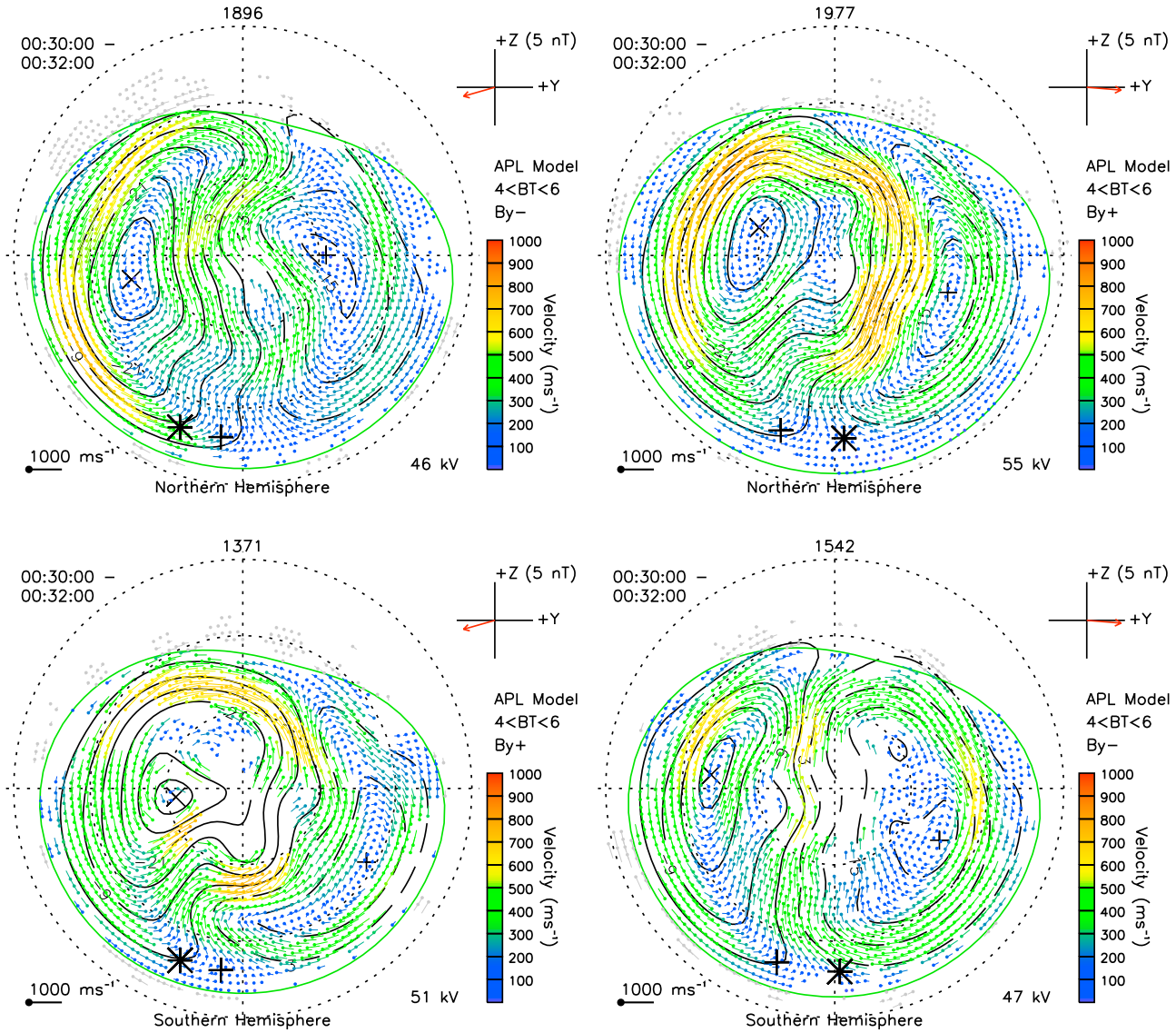

Figure 4d. Average ionospheric convection patterns from 30 mins after substorm onset.

so-called "Harang discontinuity" [*Harang*, 1946; *Heppner*, 1972; *Marghitu et al.*, 2009], a region where the eastward electrojet lies equatorward of the westward electrojet in the same longitudinal plane. This feature, which is manifest in our data as the "double reversal" discussed in section 3, has been studied in the past using magnetohydrodynamic (MHD) simulations [e.g., *Tanaka*, 2001] and empirical models [e.g., *Heppner and Maynard*, 1987; *Weimer*, 1999] and is suggested to be caused by the synthesized effect of magnetospheric driving by the solar wind and nonuniform ionospheric conductivity. This is consistent with our results in the sense that the portion of the convection patterns that appears to deviate from the expected IMF B_Y-control coincides with the nightside auroral zone where strong ionospheric conductivity gradients are likely to exist. In the study by *Weimer* [1999] Dynamics Explorer (DE)-2 observations were used specifically to distinguish the substorm and nonsubstorm time components of the ionospheric convection patterns. However, *Weimer* [1999] defined substorms using only the AE indices such that no time-evolution was preserved in the analysis. In addition, his nonsubstorm group would have included substorm growth phase intervals during which, according to [*Zou et al.*, 2009], the substorm electrodynamics are already starting to develop. In this study by *Zou et al.* [2009] the evolution of the Harang discontinuity was investigated in more detail and was found to develop in concert with the subauroral polarisation streams (SAPS) [*Foster and Burke*, 2002] and associated region 2 current system. This study also revealed that substorm onset tends to occur within the flow reversal region of the Harang discontinuity implying to some extent that the onset location is predetermined, a suggestion confirmed by *Milan et al.* [2010] who found a preexisting auroral emission in IMAGE FUV satellite data in the local time sector in which onset subsequently takes place. In the study by *Zou et al.* [2009], however, no reference is made to the influence of IMF B_Y in determining the onset location, nor to the direct effect of IMF B_Y on the evolution of the flows.

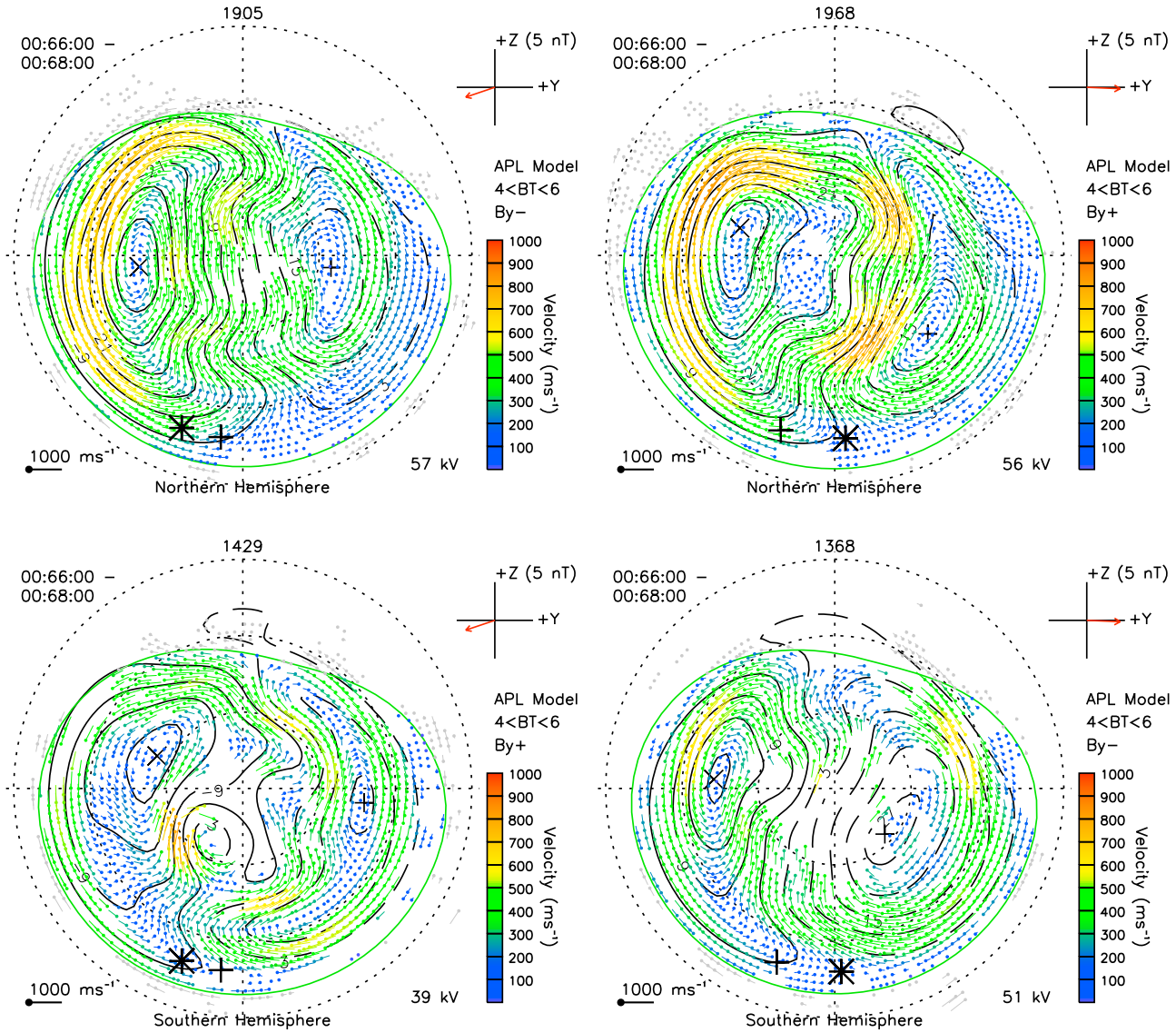

Figure 4e. Average ionospheric convection patterns from 66 mins after substorm onset.

[17] The preconditioning of the magnetosphere implied by the results of *Zou et al.* [2009] and *Milan et al.* [2010] is nevertheless apparent in our data. If we consider the convection patterns in Figures 4a–4c then it is the patterns in Figures 4b and 4c that look the most similar, despite the fact that Figures 4a and 4b are during the growth phase and only Figure 4c at onset. This suggests that by ~15 mins prior to onset the nightside auroral zone convection is already developing, in "anticipation" of the substorm onset to follow. However, our results suggest that it is not simply a case of the prevailing IMF B_Y governing the local time development of the auroral zone electrodynamics. Certainly, there is some evidence that IMF B_Y governs the local time of substorm onset, but it seems that the substorm exhibits its own intrinsic dusk-dawn asymmetry which is, to some extent, independent of the IMF conditions or, at least, not directly related in the simple way observed on the dayside. Consider, for example, the statistical patterns of *Ruohoniemi and Greenwald* [2005], illustrated in Figure 1. Here we can see some evidence for the Harang discontinuity in the positive IMF B_Y case, presumably owing to the effect of some substorms being present in their statistics. The average pattern for the negative B_Y case, however, shows no such evidence. The fact that it is evident for some IMF orientations but not others suggests that the extent to which the IMF controls the convection pattern is not the same as the extent to which it is controlling the substorm electrodynamics.

[18] To illustrate the relationship between IMF and substorm controlled convection we show in Figure 5 a schematic depicting the primary differences between the nature of the convection pattern driven by tail reconnection during substorm and nonsubstorm times, for different prevailing IMF B_Y orientations. In Figure 5 (top), we show the case for nonsubstorm times, where the basic shape of the patterns

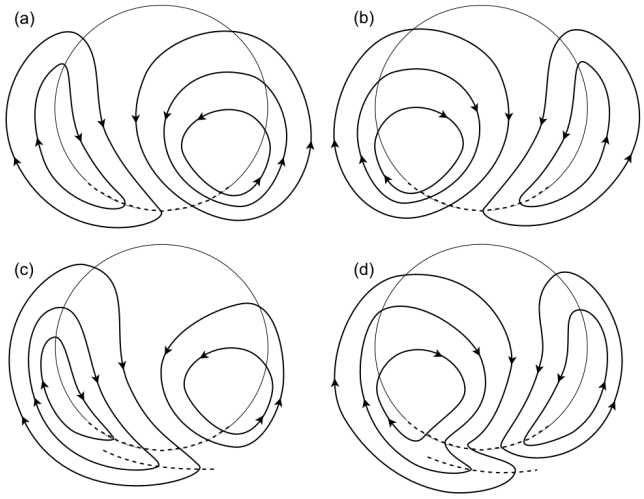

Figure 5. A schematic depicting the primary differences between the nature of the ionospheric convection pattern driven by tail reconnection during (a and b) nonsubstorm and (c and d) substorm times, for different prevailing IMF B_Y orientations: (a and c) northern (southern) hemisphere $B_Y < 0$ ($B_Y > 0$) and (b and d) northern (southern) hemisphere $B_Y > 0$ ($B_Y < 0$). In Figures 5a–5d, the circle represents the open-closed field line boundary, and the dashed portion the ionospheric projection of the tail reconnection line. The arrowed curves then represent the streamlines of plasma convection excited in the ionosphere.

resembles those discussed by, for example, *Lockwood* [1991]. The circle represents the open-closed field line boundary, and the dashed portion the ionospheric projection of the tail reconnection line. The arrowed curves then represent the streamlines of plasma convection excited in the ionosphere. In Figure 5 (bottom), we show the corresponding convection patterns for substorm times, illustrating the juxtaposition of the solar wind and substorm driven components of the convection pattern. Here, in the polar cap, the plasma streamlines take the same form as before, since the open field lines are still controlled by the IMF, with no "knowledge" of any substorm activity within the plasma sheet. At lower latitudes, within the auroral zone, we have drawn a second projected "near-Earth" reconnection line (although this could similarly simply represent the projected location of some current instability within the plasma sheet). In this region, rather than being directly controlled by the prevailing IMF conditions, the flows are dominated by the substorm electrodynamics. This is consistent with the findings of *Zou et al.* [2009] who found the substorm dynamics to be closely associated with nightside region 2 physics. It is also consistent with the "double branch" auroral configuration [e.g., *Elphinstone et al.*, 1995] that is typically activated 20 min after substorm onset [*Sandholt et al.*, 2002].

[19] A key feature of this schematic in explaining our observations is the existence of the reconnection line at the open closed field line boundary. We suggest that, at least to some extent, reconnection of open field lines occurs here during a substorm, perhaps even beginning during the late growth phase. This is consistent with observations of intensifications of the poleward boundary of the auroral oval by *Lyons et al.* [1999] and observations of fast flows at the open-closed field line boundary a few minutes prior to onset [*Lyons et al.*, 2010]. *Nishimura et al.* [2010] suggest that new plasma crosses the polar cap boundary into the plasma sheet and then intrudes to the near-Earth region, leading to onset. Whilst this may be true, it is also reasonable to suggest that some of this newly reconnected flux cannot penetrate into the near-Earth plasma sheet due to flux pileup and instead gets diverted around the flanks. This could explain the higher-latitude channel of return flow in the convection patterns discussed in section 3. If these IMF B_Y-carrying field lines are closing at a more distant reconnection line and returning to the dayside at higher latitudes rather than penetrating deeper into the plasma sheet this could also explain the lack of (or at least reduced) IMF B_Y-control of the inner magnetosphere where the substorm instability is developing. Where the substorm-driven dusk-dawn asymmetry happens to match that in the polar cap (determined by the IMF B_Y) we get the resultant convection pattern shown in Figure 5c, whereas when the opposite sense of IMF B_Y is present in the polar cap relative to the asymmetry within the auroral zone, the convection forms the "double reversal" shown in Figure 5d.

[20] As an additional check on the lack of IMF B_Y-control of the substorm auroral convection we produced a supplemental set of northern hemisphere superposed epoch average convection patterns, further restricting our selection criteria such that only substorms with onset MLTs in the ranges 20–22 h and 00–02 h were included. We show one example of this analysis in Figure 6, which consists of two average convection patterns from 20 mins after substorm onset presented in a similar format to Figure 4. In Figure 6 (left) we show the N− pattern, for substorms with onset MLTs in the range 20–22 h and in Figure 6 (right) the N+ pattern for substorms with onset MLTs in the range 00–02 h. These data clearly illustrate the lack of IMF B_Y-control in the nightside auroral zone. On the dayside each pattern exhibits the expected B_Y asymmetry, yet on the nightside the dusk-dawn asymmetry is exactly the opposite to that associated with IMF B_Y in the absence of substorms. Instead, it appears to be the location of the Harang discontinuity that is governing the orientation of the nightside flows. As discussed by *Zou et al.* [2009] the evolution of the Harang is closely related to the MLT of the substorm onset. In the case that this is postmidnight (Figure 6 (right)) the Harang is clearly present, in apparent contradiction with the expected IMF B_Y-asymmetry. In the premidnight onset case (Figure 6 (left)) there is no evidence for the Harang at all yet its influence is implied by the existence of a dusk-dawn asymmetry that is again exactly opposite to that which would be produced by the influence of IMF B_Y.

[21] Finally, it is worth noting that we are not precluding the idea of IMF B_Y-control of substorm electrodynamics in the above argument, but rather a lack of the direct control that is observed on the dayside. Indeed, *Milan et al.* [2010] suggest that for one sense of B_Y to dominate in the magnetotail during substorms it must have persisted in the solar wind for the previous 2 to 3 growth phases. It is quite possible, therefore, that it is simply the timescales that differ between the IMF influence on the dayside and polar cap

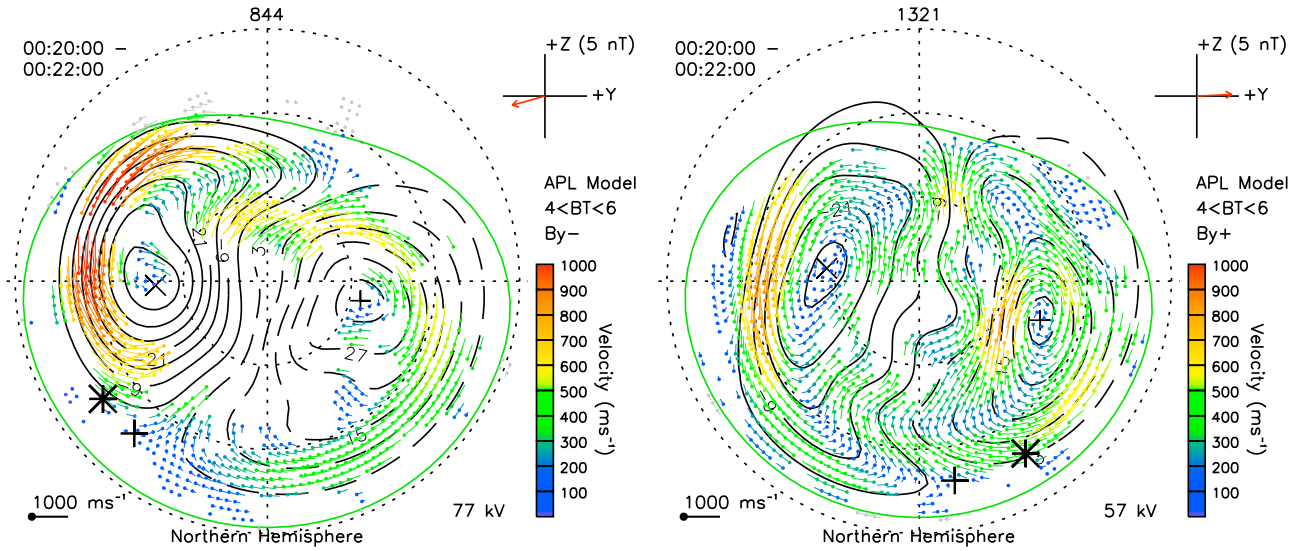

Figure 6. Average ionospheric convection patterns from the northern hemisphere, in a similar format to Figure 4, from 20 mins after substorm onset. (left) Substorms that had their onset between 20 and 22 MLT. (right) Substorms that had their onset between 00 and 02 MLT.

convection, and its influence on the substorm dynamics. It might be interesting to investigate this hypothesis in future work by repeating the present study, not with isolated substorms, but with intervals of extended substorm activity occurring under steady IMF conditions. It might also be instructive to further investigate the relationship between the convection evolution and that of the auroral emission discussed by *Milan et al.* [2010].

5. Summary

[22] We have presented superposed epoch analyses of the average ionospheric convection response to magnetospheric substorms occurring under different orientations of IMF B_Y. Our results show that although the orientation of the IMF strongly governs the nature of the coupled magnetosphere-ionosphere convection during the growth phase, during the expansion phase the expected dusk-dawn asymmetry is retained only in the polar cap and dayside auroral zone. In the nightside auroral zone the convection is reordered according to the local substorm electrodynamics with any remaining asymmetry being more closely related to the magnetic local time of substorm onset. Owing to the preponderance of substorms occurring just prior to magnetic midnight, the substorm-driven dusk-dawn asymmetry tends to be an azimuthal extension of the dusk convection cell across the midnight sector, a manifestation of the so-called "Harang discontinuity". This results in the northern (southern) hemisphere nightside auroral convection during substorms generally conforming to the expected pattern for negative (positive) IMF B_Y. When the opposite IMF B_Y-driven convection pattern preexists the nightside auroral convection changes markedly over the course of the substorm to establish this same "Harang" configuration. Additional, smaller-scale asymmetries are also apparent between the northern and southern hemispheres. We anticipate that studies currently in progress using all-sky imager data in conjunction with higher spatial resolution radar observations will elucidate the cause of these interhemispheric anomalies.

[23] **Acknowledgments.** We would like to thank the PIs of the SuperDARN radars for provision of the radar data and R. J. Barnes of the Johns Hopkins University for the "Map-Potential" algorithm. We also thank the ACE MAG and SWEPAM instrument teams and the ACE Science Center for providing the ACE data, and Harald Frey for providing the IMAGE FUV substorm database. This work was partly supported by the Inter-university Upper atmosphere Global Observation NETwork (IUGONET) project funded by the Ministry of Education, Culture, Sports, Science and Technology (MEXT), Japan. AG, ETS and TKY were supported during this study by STFC grant PP/E000983/1, and JAW by STFC grant PP/E001947/1. SuperDARN operations at the University of Leicester are supported by STFC grant PP/E007929/1.

[24] Robert Lysak thanks the reviewers for their assistance in evaluating this paper.

References

Baker, D. N., T. I. Pulkkinen, V. Angelopoulos, W. Baumjohann, and R. L. McPherron (1996), Neutral line model of substorms: Past results and present view, *J. Geophys. Res.*, *101*, 12,975–13,010, doi:10.1029/95JA03753.

Baker, K. B., and S. Wing (1989), A new magnetic coordinate system for conjugate studies at high-latitudes, *J. Geophys. Res.*, *94*(A7), 9139–9143, doi:10.1029/JA094iA07p09139.

Bristow, W. A., and P. Jensen (2007), A superposed epoch study of SuperDARN convection observations during substorms, *J. Geophys. Res.*, *112*, A06232, doi:10.1029/2006JA012049.

Chisham, G., et al. (2007), A decade of the Super Dual Auroral Radar Network (SuperDARN): scientific achievements, new techniques and future directions, *Surv. Geophys.*, *28*, 33–109, doi:10.1007/s10712-007-9017-8.

Cowley, S. W. H. (1981), Magnetospheric asymmetries associated with the Y-component of the IMF, *Planet. Space Sci.*, *29*(1), 79–96.

Cowley, S. W. H., and M. Lockwood (1992), Excitation and decay of solar wind-driven flows in the magnetosphere-ionosphere system, *Ann. Geophys.*, *10*, 103–115.

Cowley, S. W. H., and M. Lockwood (1996), Time-dependent flows in the coupled solar wind-magnetosphere-ionosphere system, *Adv. Space Res.*, *18*, 141–150.

Dungey, J. W. (1961), Interplanetary magnetic field and the auroral zones, *Phys. Rev. Lett.*, *6*, 47–48, doi:10.1103/PhysRevLett.6.47.

Elphinstone, R. D., et al. (1995), The double oval UV auroral distribution. 2. The most poleward arc system and the dynamics of the magnetotail, *J. Geophys. Res.*, *100*(A7), 12,093–12,102.

Etemadi, A., S. W. H. Cowley, M. Lockwood, B. J. I. Bromage, D. M. Willis, and H. Luhr (1988), The dependence of high-latitude dayside ionospheric flows on the north south component of the IMF—A high time resolution correlation-analysis using EISCAT POLAR and AMPTE UKS and IRM data, *Planet. Space Sci.*, *36*(5), 471–498.

Fairfield, D. H. (1977), Electric and magnetic-fields in high latitude magnetosphere, *Rev. Geophys.*, *15*(3), 285–298.

Foster, J. C., and W. J. Burke (2002), SAPS: A new characterization for sub-auroral electric fields, *Eos Trans. AGU*, *83*, 393–394.

Freeman, M. P., and D. J. Southwood (1988), The effect of magnetospheric erosion on mid-latitude and high-latitude ionospheric flows, *Planet. Space Sci.*, *36*(5), 509–522.

Frey, H. U., S. B. Mende, V. Angelopoulos, and E. F. Donovan (2004), Substorm onset observations by IMAGE-FUV, *J. Geophys. Res.*, *109*, A10304, doi:10.1029/2004JA010607.

Greenwald, R. A., et al. (1995), Darn/SuperDarn: A global view of the dynamics of high-latitude convection, *Space Sci. Rev.*, *71*, 761–796, doi:10.1007/BF00751350.

Grocott, A., S. W. H. Cowley, J. B. Sigwarth, J. F. Watermann, and T. K. Yeoman (2002), Excitation of twin-vortex flow in the nightside high-latitude ionosphere during an isolated substorm, *Ann. Geophys.*, *20*, 1577–1601.

Grocott, A., S. W. H. Cowley, and J. B. Sigwarth (2003), Ionospheric flow during extended intervals of northward but B_Y-dominated IMF, *Ann. Geophys.*, *21*, 509–538.

Grocott, A., T. K. Yeoman, S. E. Milan, and S. W. H. Cowley (2005), Interhemispheric observations of the ionospheric signature of tail reconnection during IMF-northward non-substorm intervals, *Ann. Geophys.*, *23*, 1763–1770.

Grocott, A., M. Lester, M. L. Parkinson, T. K. Yeoman, P. L. Dyson, J. C. Devlin, and H. U. Frey (2006), Towards a synthesis of substorm electrodynamics: HF radar and auroral observations, *Ann. Geophys.*, *24*, 3365–3381.

Grocott, A., T. K. Yeoman, S. E. Milan, O. Amm, H. U. Frey, L. Juusola, R. Nakamura, C. J. Owen, H. Rème, and T. Takada (2007), Multi-scale observations of magnetotail flux transport during IMF-northward non-substorm intervals, *Ann. Geophys.*, *25*, 1709–1720.

Grocott, A., S. E. Milan, and T. K. Yeoman (2008), Interplanetary magnetic field control of fast azimuthal flows in the nightside high-latitude ionosphere, *Geophys. Res. Lett.*, *35*, L08102, doi:10.1029/2008GL033545.

Grocott, A., J. A. Wild, S. E. Milan, and T. K. Yeoman (2009), Superposed epoch analysis of the ionospheric convection evolution during substorms: Onset latitude dependence, *Ann. Geophys.*, *27*(2), 591–600.

Harang, L. (1946), The mean field of disturbance of polar geomagnetic storms, *Terr. Magn. Atmos. Electr.*, *51*(3), 353–380, doi:10.1029/TE051i003p00353.

Heppner, J. P. (1972), The Harang discontinuity in auroral belt ionospheric currents, *Geophys. Norv.*, *29*, 105–120.

Heppner, J. P., and N. C. Maynard (1987), Empirical high-latitude electric-field models, *J. Geophys. Res.*, *92*(A5), 4467–4489.

Jørgensen, T. S., E. Friis-Christensen, and J. Wilhjelm (1972), Interplanetary magnetic-field direction and high latitude ionospheric currents, *J. Geophys. Res.*, *77*(10), 1976–1977.

Liou, K., and J. Ruohoniemi (2006a), A case study of relationship between substorm expansion and global plasma convection, *Geophys. Res. Lett.*, *33*, L02105, doi:10.1029/2005GL024736.

Liou, K., and J. Ruohoniemi (2006b), Correction to "A case study of relationship between substorm expansion and global plasma convection", *Geophys. Res. Lett.*, *33*, L10101, doi:10.1029/2006GL025990.

Lockwood, M. (1991), Modelling the high-latitude ionosphere, in *Proceedings IEE Colloqium on "National Radio Propagation Programme"*, p. 10, IEE, London.

Lyons, L., T. Nagai, G. Blanchard, J. Samson, T. Yamamoto, T. Mukai, A. Nishida, and S. Kokubun (1999), Association between Geotail plasma flows and auroral poleward boundary intensifications observed by CANOPUS photometers, *J. Geophys. Res.*, *104*(A3), 4485–4500.

Lyons, L. R., J. M. Ruohoniemi, and G. Lu (2001), Substorm-associated changes in large-scale convection during the November 24, 1996 Geospace Environment Modeling event, *J. Geophys. Res.*, *106*, 397–406, doi:10.1029/1999JA000602.

Lyons, L. R., Y. Nishimura, Y. Shi, S. Zou, H. J. Kim, V. Angelopoulos, C. Heinselman, M. J. Nicolls, and K. H. Fornacon (2010), Substorm triggering by new plasma intrusion: Incoherent-scatter radar observations, *J. Geophys. Res.*, *115*, A07223, doi:10.1029/2009JA015168.

Marghitu, O., T. Karlsson, B. Klecker, G. Haerendel, and J. P. McFadden (2009), Auroral arc and oval electrodynamics in the Harang region, *J. Geophys. Res.*, *114*, A03214, doi:10.1029/2008JA013630.

Mende, S. B., et al. (2000a), Far ultraviolet imaging from the IMAGE spacecraft. 2. Wideband FUV imaging, *Space Sci. Rev.*, *91*, 271–285.

Mende, S. B., et al. (2000b), Far ultraviolet imaging from the IMAGE spacecraft. 1. System design, *Space Sci. Rev.*, *91*, 243–270.

Milan, S. E., M. Lester, S. W. H. Cowley, K. Oksavik, M. Brittnacher, R. A. Greenwald, G. Sofko, and J.-P. Villain (2003), Variations in the polar cap area during two substorm cycles, *Ann. Geophys.*, *21*(5), 1121–1140.

Milan, S. E., B. Hubert, and A. Grocott (2005), Formation and motion of a transpolar arc in response to dayside and nightside reconnection, *J. Geophys. Res.*, *110*, A01212, doi:10.1029/2004JA010835.

Milan, S. E., A. Grocott, C. Forsyth, S. M. Imber, P. D. Boakes, and B. Hubert (2009), A superposed epoch analysis of auroral evolution during substorm growth, onset and recovery: open magnetic flux control of substorm intensity, *Ann. Geophys.*, *27*(2), 659–668.

Milan, S. E., A. Grocott, and B. Hubert (2010), A superposed epoch analysis of auroral evolution during substorms: Local time of onset region, *J. Geophys. Res.*, *115*, A00I04, doi:10.1029/2010JA015663.

Morelli, J. P., et al. (1995), Radar observations of auroral zone flows during a multiple-onset substorm, *Ann. Geophys.*, *13*, 1144–1163.

Nishida, A., T. Mukai, T. Yamamoto, Y. Saito, S. Kokubun, and K. Maezawa (1995), Geotail observation of magnetospheric convection in the distant tail at 200 R_E in quiet times, *J. Geophys. Res.*, *100*(A12), 23,663–23,675.

Nishida, A., T. Mukai, T. Yamamoto, S. Kokubun, and K. Maezawa (1998), A unified model of the magnetotail convection in geomagnetically quiet and active times, *J. Geophys. Res.*, *103*(A3), 4409–4418.

Nishimura, Y., L. R. Lyons, S. Zou, V. Angelopoulos, and S. Mende (2010), Substorm triggering by new plasma intrusion: THEMIS all-sky imager observations, *J. Geophys. Res.*, *115*, A07222, doi:10.1029/2009JA015166.

Østgaard, N., S. Mende, H. Frey, T. Immel, L. Frank, J. Sigwarth, and T. Stubbs (2004), Interplanetary magnetic field control of the location of substorm onset and auroral features in the conjugate hemispheres, *J. Geophys. Res.*, *109*, A07204, doi:10.1029/2003JA010370.

Østgaard, N., S. B. Mende, H. U. Frey, J. B. Sigwarth, A. Asnes, and J. M. Weygand (2007), Auroral conjugacy studies based on global imaging, *J. Atmos. Sol. Terr. Phys.*, *69*(3), 249–255, doi:10.1016/j.jastp.2006.05.026.

Parker, E. N. (1963), *Interplanetary Dynamical Processes*, Interscience, New York.

Provan, G., M. Lester, S. Mende, and S. Milan (2004), Statistical study of high-latitude plasma flow during magnetospheric substorms, *Ann. Geophys.*, *22*, 3607–3624.

Provan, G., M. Lester, A. Grocott, and S. Cowley (2005), Pulsed flows observed during an interval of prolonged northward IMF, *Ann. Geophys.*, *23*(4), 1207–1225.

Ruohoniemi, J. M., and K. B. Baker (1998), Large-scale imaging of high-latitude convection with Super Dual Auroral Radar Network HF radar observations, *J. Geophys. Res.*, *103*, 20,797–20,811, doi:10.1029/98JA01288.

Ruohoniemi, J. M., and R. A. Greenwald (1996), Statistical patterns of high-latitude convection obtained from Goose Bay HF radar observations, *J. Geophys. Res.*, *101*, 21,743–21,764, doi:10.1029/96JA01584.

Ruohoniemi, J. M., and R. A. Greenwald (1998), The response of high-latitude convection to a sudden southward IMF turning, *Geophys. Res. Lett.*, *25*(15), 2913–2916, doi:10.1029/98GL02212.

Ruohoniemi, J. M., and R. A. Greenwald (2005), Dependencies of high-latitude plasma convection: Consideration of interplanetary magnetic field, seasonal, and universal time factors in statistical patterns, *J. Geophys. Res.*, *110*, A09204, doi:10.1029/2004JA010815.

Ruohoniemi, J. M., R. A. Greenwald, O. de la Beaujardière, and M. Lester (1993), The response of the high-latitude dayside ionosphere to an abrupt northward transition in the IMF, *Ann. Geophys.*, *11*(7), 544–555.

Sandholt, P. E., and C. J. Farrugia (2007), Poleward moving auroral forms (PMAFs) revisited: Responses of aurorae, plasma convection and Birkeland currents in the pre- and postnoon sectors under positive and negative IMF B_Y conditions, *Ann. Geophys.*, *25*(7), 1629–1652.

Sandholt, P. E., and C. J. Farrugia (2009), Plasma flow channels at the dawn/dusk polar cap boundaries: momentum transfer on old open field lines and the roles of IMF B_Y and conductivity gradients, *Ann. Geophys.*, *27*(4), 1527–1554.

Sandholt, P. E., C. J. Farrugia, J. Moen, and S. W. H. Cowley (1998a), Dayside auroral configurations: Responses to southward and northward rotations of the interplanetary magnetic field, *J. Geophys. Res.*, *103*(A9), 20,279–20,295.

Sandholt, P. E., C. J. Farrugia, J. Moen, O. Noraberg, B. Lybekk, T. Sten, and T. Hansen (1998b), A classification of dayside auroral forms and activities as a function of interplanetary magnetic field orientation, *J. Geophys. Res.*, *103*(A10), 23,325–23,345.

Sandholt, P. E., C. J. Farrugia, M. Lester, S. W. H. Cowley, S. E. Milan, W. F. Denig, B. Lybekk, E. Trondsen, and V. Vorobjev (2002), Multistage substorm expansion: Auroral dynamics in relation to plasma sheet particle injection, precipitation, and plasma convection, *J. Geophys. Res.*, *107*(A11), 1342, doi:10.1029/2001JA900116.

Sandholt, P. E., Y. Andalsvik, and C. J. Farrugia (2010), Polar cap convection/precipitation states during Earth passage of two ICMEs at solar minimum, *Ann. Geophys.*, *28*(4), 1023–1042.

Shepherd, S., and J. Ruohoniemi (2000), Electrostatic potential patterns in the high-latitude ionosphere constrained by SuperDARN measurements, *J. Geophys. Res.*, *105*(A10), 23,005–23,014.

Siscoe, G. L., and T. S. Huang (1985), Polar-cap inflation and deflation, *J. Geophys. Res.*, *90*(A1), 543–547, doi:10.1029/JA090iA01p00543.

Smith, C. W., J. L'Heureux, N. F. Ness, M. H. Acuña, L. F. Burlaga, and J. Scheifele (1998), The ACE magnetic fields experiment, *Space Sci. Rev.*, *86*, 613–632, doi:10.1023/A:1005092216668.

Stone, E. C., A. M. Frandsen, R. A. Mewaldt, E. R. Christian, D. Margolies, J. F. Ormes, and F. Snow (1998), The Advanced Composition Explorer, *Space Sci. Rev.*, *86*, 1–22, doi:10.1023/A:1005082526237.

Svalgaard, L. (1973), Polar-cap magnetic variations and their relationship with interplanetary magnetic sector structure, *J. Geophys. Res.*, *78*(13), 2064–2078.

Tanaka, T. (2001), Interplanetary magnetic field B_Y and auroral conductance effects on high-latitude ionospheric convection patterns, *J. Geophys. Res.*, *106*(A11), 24,505–24,516.

Todd, H., S. W. H. Cowley, M. Lockwood, D. M. Wills, and H. Luhr (1988), Response-time of the high-latitude dayside ionosphere to sudden changes in the north-south component of the IMF, *Planet. Space Sci.*, *36*(12), 1415–1428.

Wang, H., H. Lühr, and A. J. Ridley (2010), Plasma convection jets near the poleward boundary of the nightside auroral oval and their relation to Pedersen conductivity gradients, *Ann. Geophys.*, *28*(4), 969–976.

Watanabe, M., N. Sato, R. A. Greenwald, M. Pinnock, M. R. Hairston, R. L. Rairden, and D. J. McEwen (2000), The ionospheric response to interplanetary magnetic field variations: Evidence for rapid global change and the role of preconditioning in the magnetosphere, *J. Geophys. Res.*, *105*(A10), 22,955–22,977.

Weimer, D. R. (1999), Substorm influence on the ionospheric electric potentials and currents, *J. Geophys. Res.*, *104*, 185–198, doi:10.1029/1998JA900075.

Wild, J. A., and A. Grocott (2008), The influence of magnetospheric substorms on SuperDARN radar backscatter, *J. Geophys. Res.*, *113*, A04308, doi:10.1029/2007JA012910.

Yeoman, T. K., J. A. Davies, N. M. Wade, G. Provan, and S. E. Milan (2000a), Combined CUTLASS, EISCAT and ESR observations of ionospheric plasma flows at the onset of an isolated substorm, *Ann. Geophys.*, *18*, 1073–1087.

Yeoman, T. K., R. V. Lewis, H. Khan, S. W. H. Cowley, and J. M. Ruohoniemi (2000b), Interhemispheric observations of nightside ionospheric electric fields in response to IMF B_Z and B_Y changes and substorm pseudobreakup, *Ann. Geophys.*, *18*(8), 897–907.

Yu, Y. Q., and A. J. Ridley (2009), Response of the magnetosphere-ionosphere system to a sudden southward turning of interplanetary magnetic field, *J. Geophys. Res.*, *114*, A03216, doi:10.1029/2008JA013292.

Zou, S., L. R. Lyons, C. P. Wang, A. Boudouridis, J. M. Ruohoniemi, P. C. Anderson, P. L. Dyson, and J. C. Devlin (2009), On the coupling between the harang reversal evolution and substorm dynamics: A synthesis of SuperDARN, DMSP, and IMAGE observations, *J. Geophys. Res.*, *114*, A01205, doi:10.1029/2008JA013449.

A. Grocott, S. E. Milan, and T. K. Yeoman, Department of Physics and Astronomy, University of Leicester, University Road, Leicester LE1 7RH, UK. (a.grocott@ion.le.ac.uk)

N. Sato and A. S. Yukimatu, Space and Upper Atmospheric Sciences Research Group, National Institute of Polar Research, Research Organization of Information and Systems, 10-3, Midoricho, Tachikawa, Tokyo 190-8518, Japan.

J. A. Wild, Department of Physics, Lancaster University, Lancaster LA1 4YB, UK.